https://dx.doi.org/10.4314/dujopas.v10i2a.3
ISSN (Print): 2476-8316
ISSN (Online): 2635-3490
Dutse Journal of Pure and Applied Sciences (DUJOPAS), *Vol. 10 No. 2a June 2024*

Yield Optimization of Chemically Synthesized p-TSA-Doped Polyaniline using a Box-Behnken Design of Experiment

Shehu Umar[1*], Ahmad Uba[2], Chika Muhammad[1], Thompson Izuagie[3] and Abdullahi Isah[4]

[1]Department of Energy and Applied Chemistry,
Usmanu Danfodiyo University
Sokoto.

[2]Department of Pharmaceutical and Medicinal Chemistry,
Usmanu Danfodiyo University
Sokoto.

[3]Department of Chemistry,
Sokoto State University.

[4]Department of Science Laboratory Technology,
Umaru Ali Shinkafi Polytechnic
Sokoto.

Email: shehumar07@gmail.com

Abstract

This research was aimed at optimizing the polyaniline (PAni) yield using a Box-Behnken design of experiment (DOE). The PAni sample was synthesized by the oxidative chemical polymerization of aniline using p-toluene sulfonic acid (p-TSA) as the dopant acid and ammonium peroxydisulfate (APS) as the initiator. The factors (concentration of dopant acid, initiator-to-monomer ratio, and the addition rate of initiator to monomer) that affect the yield were varied using a Box-Behnken DOE method. The polymer was characterized using various analytical techniques, including Ultraviolet-visible spectroscopy (UV-Vis), Fourier-transform infrared spectroscopy (FTIR), x-ray diffraction (XRD), and scanning electron microscopy (SEM). The yield was calculated and examined using the regression equation, main effects plots, contour plots, and optimisation plots. The results show that under the optimized conditions of dopant acid concentration of 0.1 mol/dm^3, an initiator addition rate of 45 cm^3/h, and an initiator to monomer (I/M) ratio of 1.5, PAni with a yield of 82.81% was obtainable. The characteristics identified in the UV-Vis analysis confirm that the synthesized PAni exhibits a semi-conductive property and as a result, could be applied as an additive in anticorrosive paint.

Keywords: chemical synthesis, polyaniline, p-TSA dopant, yield optimization, band gap energy.

Author for Correspondence

INTRODUCTION

There is currently, an increasing trend in the use of polymers in conducting and/or semiconducting applications (Luscombe *et al.,* 2021; Sharma *et al.,* 2021; Haldhar, *et al*., 2022). In the marine world, scientists create graphene-based polymer coatings that shield the metal from the ravages of saltwater (Sharma & Sharma, 2023). Their strength, conductivity, and expansive surface area make them exceptional barriers against corrosion. Polymers also excel in safeguarding delicate electronics. Researchers have shown that epoxy resin coatings infused with polyaniline (PAni) offer remarkable protection for mild steel components, preventing internal damage that can cripple electronic devices (Ulaeto *et al.,* 2023). Synthetic polymers or plastics, in general, have a high electrical resistivity and are widely used as electrical cable insulation. Whereas doped polymers can exhibit electrical conductivity (Sharma *et al.*, 2021). For example, PAni is an important conducting polymer because of its high conductivity in a doped state (Sharma *et al.*, 2021). The polymer's ability to carry electrical charge is attributed to the presence of conjugated π electrons formed by single and double bonds in the polymer's backbone or ring structure, and the introduction of dopants results in an imbalance of electrons (Li, 2018). The degree of conjugated conductive polymer structure allows the new electron population to move around the backbone when an electric potential is applied (Li, 2018).

In general, conductivity increases with decreasing band gap (Aizamddin *et al.*, 2020). The band gap represents the minimum energy required for lifting an electron from the valence band to the conduction band, with metals displaying no band gap, while numerous insulators like polymers exhibit a substantial band gap ranging from 1.5 to 4eV (Khalid *et al.*, 2011). This wide band gap obstructs electron flow; however, by carefully designing the polymer backbone's chemical structure, a band gap as low as 0.5 to 1 eV can be achieved (Khalid *et al.*, 2011). An early explanation of conducting polymers was based on band theory as a method of construction (Mishra *et al.* 2018). The theory postulates that valence bands are half-filled because of a continuous delocalized π system, which would be optimal for conducting electricity. Nevertheless, the polymer demonstrates the ability to reduce its energy through band modification, resulting in a 1.5eV bandwidth, classifying it as a semiconductor with a high energy gap.

Doping the polymer with either an electron donor or an electron acceptor could result in its transformation into a conducting Material Mishra *et al.* (2018). Bavane (2014) had earlier noted that the free spin concentration increases as the concentration of dopant is increased. This concept has been succinctly described to involve the mechanisms of charge storage mechanisms along the polymer chain by Mishra *et al.* (2018).

In the present study, polyaniline has been prepared by chemical polymerization using p-TSA as dopant acid and aniline monomer at different concentration ratios. The polymer yield was optimized using the Box Behnken design of the experiment.

MATERIALS AND METHODS

MATERIALS

Analytical grade Acetone (99%, BDH), Ammonium peroxydisulfate (99%, Sigma Aldrich), aniline (99.5%, Sigma Aldrich), Methanol (99.8%, Sigma Aldrich), and *p*-Toluene sulfonic acid (98%, BDH) were used in this research work.

Synthesis of Polyaniline Doped p-Toluene Sulfonic Acid

The polyaniline (PAni) doped p-toluene sulfonic acid (p-TSA) was synthesized by the chemical oxidative method according to the method previously described by Ratheesh and Viswanathan, (2013). Aniline monomer (1.38 cm^3) was dissolved in 150 cm^3 of 0.55 M aqueous solution of p-TSA in a round bottom flask and was placed inside an ice bath (Figure 2.1). The process was maintained at 0 – 5 ^oC and the mixture was stirred mechanically at 300 rpm for 8 hr. The initiator (0.05 M) was added to the monomer-dopant mixture using a burette at 60 cm^3/hr. After allowing the content to stand for 24 h, the formed polymer was filtered and rinsed repeated with distilled water until the filtrate became clear. The residue was subsequently rinsed with methanol to remove any residual oligomers and monomers and washed with acetone before allowing it to filter overnight. The product was then dried in an oven for 6 h at 60 ^oC to obtain a dark greenish material, which was ground into a fine powder of the emeraldine salt of PAni (Jelmy *et al.,* 2013). The ranges of the selected parameters and the different experiment details are described in Tables 2.1 and 2.2.

Optimization of Yield of Polyaniline

The yield optimization of the product was done as described in 2.2.3 by investigating the effect of dopant concentration, ammonium peroxydisulfate (APS), and the rate of initiator's addition into monomer solution on the percentage yield of PAni. Multiple syntheses were conducted but with different reaction parameter combinations. Table 2.2 shows the coding of various samples synthesized with varying quantities of monomer, dopant, initiator, and I/M ratio. The following formula was used to determine the percentage yield in terms of aniline and p-TSA concentrations (Shah *et al.,* 2019):

$$\% \text{ Yield} = \frac{\text{Weight of PANI}-\text{pTSA}}{\textit{Weight of xM ANI}+\textit{Weight of xM pTSA}}\ x\ 100 \quad \text{.....(2.1)}$$

Design of Experiments

The percentage yield of polyaniline-para toluene sulfonic acid (PAni-pTSA) was optimized using a Box-Behnken design of experiments (DOE) approach. PAni-pTSA powder was synthesized by the oxidative chemical polymerization of anilinic precursor using the aqueous pTSA solution as the dopant acid and ammonium peroxydisulfate solution in water as the initiator (Jelmy *et al*., 2013). Since the optimisation of the yield of PAni depends on three main factors, the model relates the response Y to the input parameters; Dopant concentration (X_1), Initiator-to-monomer ratio (X_2), and rate of addition of initiator (X_3) as follows:

$$Y = a_0 + a_1X_1 + a_2X_2 + a_3X_3 + a_4X_1^2 + a_5X_2^2 + a_6X_3^2 + a_7X_1X_2 + a_8X_1X_3 + a_9X_2X_3 + \varepsilon \quad (2.2)$$

the linear coefficients are denoted as a_1, a_2, and a_3, while the quadratic coefficients are represented by a_4, a_5, and a_6, and the interaction coefficients by a_7, a_8, and a_9, with ε indicating the error term. Factor levels were coded as -1 for low and 1 for high. The chosen input parameters and their respective ranges are detailed in Table 2.1.

Data Analysis

Regression analysis of variance (ANOVA), response surface, contour plots, and optimization plots were created utilizing the statistical software MINITAB 17.

Table 1: Levels of Parameters Chosen in DOE for PAni-pTSA Synthesis

Variables	Code	Design Levels	
Coded Level		Low (-1)	High (1)
Dopant Concentration (mol/dm^3)	X_1	0.1	1.0
Initiator-to-Monomer Ratio	X_2	0.5	1.5
Rate of addition (cm^3/h)	X_3	30	60

Table 2: Effect of Dopant concentration, I/M ratio, and rate of addition of initiator on Percentage Yield of PAni-pTSA

Run Order	X_1 (mol/dm^3)	X_2	X_3 (cm^3/hr)	Yield (%)
1	0.55	1.5	60	
2	0.55	0.5	60	
3	1.00	1.0	60	
4	0.55	1.5	30	
5	1.00	1.0	30	
6	0.55	1.0	45	
7	0.55	1.0	45	
8	0.10	0.5	45	
9	0.10	1.0	60	
10	0.55	0.5	30	
11	1.00	0.5	45	
12	0.10	1.5	45	
13	0.55	1.0	45	
14	0.10	1.0	30	
15	1.00	1.5	45	

Characterisation of Product

The samples were characterized using Ultraviolet-visible spectroscopy (UV-Vis), Fourier-transform infrared spectroscopy (FTIR), x-ray diffraction (XRD), and scanning electron microscopy (SEM).

Ultraviolet-Visible Spectroscopy (UV-Vis) Study

The UV-Visible spectra of samples were measured in N, N-dimethylformamide on a UV-2500PC series instrument within the wavelength range of 300 to 800 nm.

The determination of the band gap energy for the π-π* transition was done using equation 2.3 as described by Sinha *et al*. (2009).

$$Eg = \frac{1240}{\lambda} \quad \ldots\ldots\ldots(2.3)$$

Where: Eg represents the band gap energy, while λ denotes the wavelength of absorption during the π-π* transition state.

Fourier-transform Infrared Spectroscopy (FTIR) **Study**

The composition of the synthesized PAni was characterized using Fourier-transform infrared spectroscopy (FTIR) analysis of powder PAni salt in the range of 400 - 4000 cm^{-1} in KBr pellets by using a Shimadzu FTIR-8400S (Rafeeq and Khalaf, 2015).

X-ray Diffractometry

The XRD (X-ray diffractometer) patterns of PAni were achieved (with PANanalytical Emperean XRD) by using Cu Kα1 radiations (λ = 1.5406 Å), and Current of 30 mA, and a Voltage of 40 KV at a Scanning speed of 5 deg/min (Rafeeq and Khalaf, 2015).

Scanning Electron Microscopy (SEM) **Study**

To understand the morphology of the polymer, the material was subjected to scanning electron microscopy using a prox: Phenom world 800-07334 (Thermo Fisher scientific) instrument.

RESULTS AND DISCUSSION

Characterization of Synthesized PAni samples

Three representative samples of the synthesized polymer chosen from DOE were characterized using UV-Visible spectroscopy, FT-IR, XRD and SEM analysis. The results are

presented and discussed below. The experimental runs 12, 14, and 9 were coded as A, B, and F respectively.

Ultraviolet-visible spectroscopy (UV-Vis)

Figure 3.1 is the UV-Vis spectra of the prepared samples of PAni-pTSA. For samples A, B, and F, the UV spectra of doped PAni revealed two distinct absorption bands each at wavelengths 289.5 and 382, 288.5 and 369, and then 305 and 373.5 nm, respectively. The first absorption band in each sample is attributed to nitrogen excitation in the benzenoid segments (π - π* transition). The second bands are due to the polaron transition in doped PAni. As noted, the π orbital generates the valence band, whereas the π* orbital constitutes the conduction band. The band gap, which is the energy differential between the two bands determines the semiconducting polymers' electrical properties. The lower the band gap energy, the easier the π - π* electronic transition, and hence, the higher the conductivity. The calculated band gap energies for samples A, B, and F are 4.07eV, 4.28eV, and 4.29eV respectively. The calculated band gap energies are similar to those reported by Sinha *et al.* (2009) for conductivities of synthesized PAni samples. The difference in energy between the π - π* transition bands, corresponds to the absorption peaks observed at 289.5nm, 288.5nm, and 305nm in the doped PAni samples. When the band gap is relatively small, typically within the range of 0.1 to 3 eV, electrons within the material can elevate their energy levels, leading them to detach from their atomic positions and transition to higher energy states within the conduction band. Once these electrons occupy the conduction band, they contribute to the material's electrical conductivity. Additionally, the formation of holes in the valence band, resulting from the movement of electrons to the conduction band, also contributes to electrical conductivity. In essence, the transfer of charge, whether it be electrons or holes, along the polymer backbone, promotes electrical conduction.

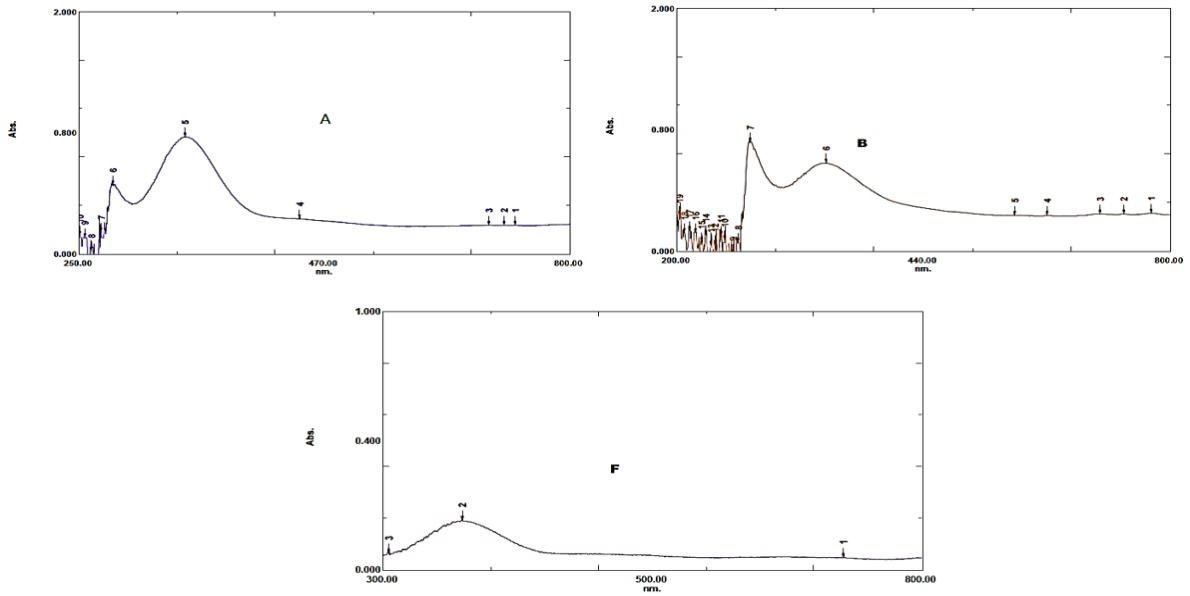

Figure 1: UV-Vis Spectra of PAni Sample A, B, and F

Fourier-Transform Infrared Spectroscopy (FTIR)

The FTIR spectra of the samples are shown in Figure 2 and Table 1 shows the distinctive peaks corresponding to each functional group for all PAni samples (A, B, and F) doped with p-TSA.

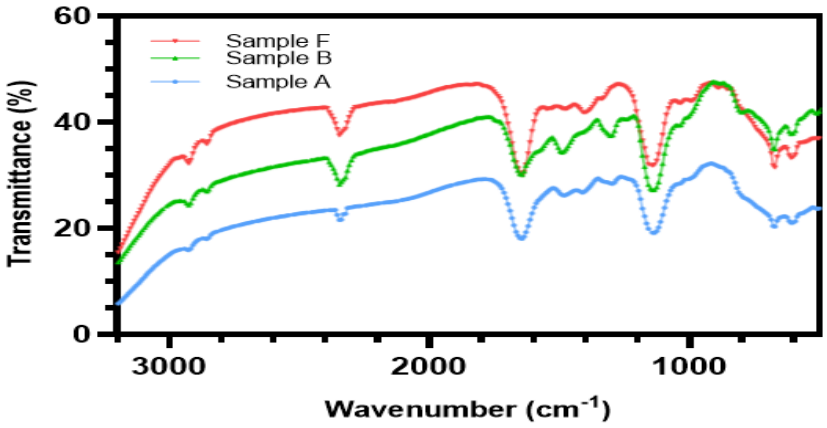

Figure 2: FTIR Spectra of different PAni Samples as Indicated

Table 1: Characteristics of wave number and Band of p-TSA doped PAni

S/N	Wave number (cm^{-1})			A_Q/A_B	Band Characteristics
	A	B	F		
1	671	671	671		C-S Benzenoid ring of p-TSA stretching
2	1033	1033	1033		O=S=O stretching of pTSA
3	1141	1141	1141		$NH^{+\cdot}$, indicating PAni is in the doped state
4	1303	1303	1303		C-N Secondary aromatic amine stretching
5	1643	1643	1643	1.11	N=Q=N Quinoid ring stretching
6	1481	1481	1481		N-B-N Benzenoid ring stretching

The FT-IR spectra (Figure 2) exhibited by the samples have almost identical peaks in the wave number range of 500 - 3500 cm^1. The spectra agree with previously published data for p-TSA doped PAni (Jelmy *et al.*, 2013; Shah *et al.*, 2019), suggesting that PAni is in a doped state. For instance, the distinct peaks of PAni at 1641 cm^1 and 1481 cm^1 were assigned to the N=Q=N stretching vibration mode of quinoid structure, and the N=B=N stretch of benzoid ring structure, respectively. The peaks at 1303 (C-N stretching), and 1141 cm^1 ($NH^{+\cdot}$ stretching), compare very well to those of the emeraldine salt form of PAni. A peak at 1033 cm^{-1} was attributed to the asymmetric and symmetric O=S=O stretching vibrations suggesting the existence of SO_3^- groups. The observation suggests the successful doping of p-TSA into the polyaniline backbone.

X-ray Diffractometry

Figure 3 depicts the XRD plots of the three PAni samples.

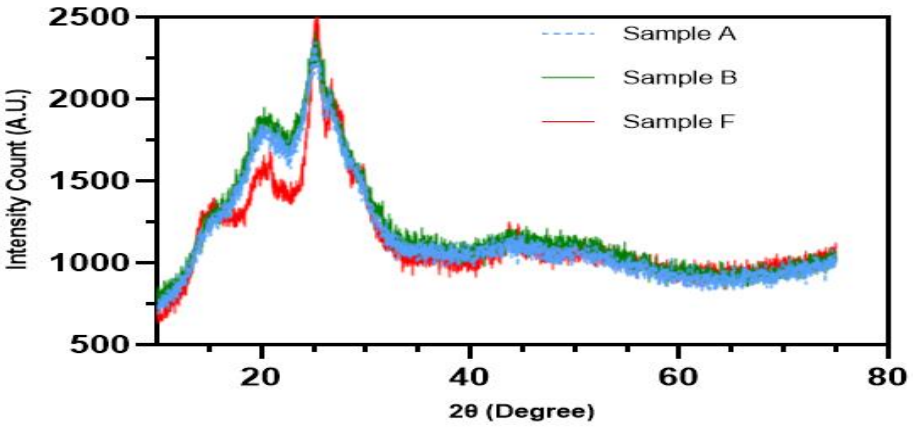

Figure 3: XRD Diffractograms of different PAni Samples as Indicated

The XRD pattern of the chemically synthesized polyaniline is given in Figure 3. The 2θ values at 15°, 20°, and 25° were ascribed to the characteristic PAni reflections, which consisted of amorphous peaks at 20° and 15° and crystalline peak at 25°. In all samples, the crystalline peak observed at 25° degrees exhibited greater prominence compared to the amorphous peaks. Furthermore, the peak at 25° indicated the extent of π conjugation in the polyaniline. The sharpness of this peak shows the longest order of π conjugation. Doped polyaniline is considered as the polymer cation-anion complex here, and polyaniline could be treated as a poly-cation while TSA^- acts as an anion that allows an increase in interchain packing and thus higher structural order, which is similar to the accepted results for HCl doped polyaniline indicating the doped state of the polyaniline (Ratheesh and Viswanathan, 2014). It was discovered that polymers with high conductivity have a higher peak intensity at 2θ than polymers with low conductivity. As a consequence, it appears that crystallinity and PAni conductivity are related. The peak's high intensity at a 2θ value of 25° suggests that the sample has a more compact molecular arrangement, resulting in good conductivity property due to a robust intramolecular electron transfer and intermolecular hopping of charge carriers.

Scanning Electron Microscopy

Figure 3.4 shows the morphology of the polymer produced. The SEM analysis was conducted on the polymer to find the effect of morphology on the coating system's anti-corrosive properties. As shown in Figure 3.4, SEM analysis of the three samples showed that they all have an agglomerates-like structure.

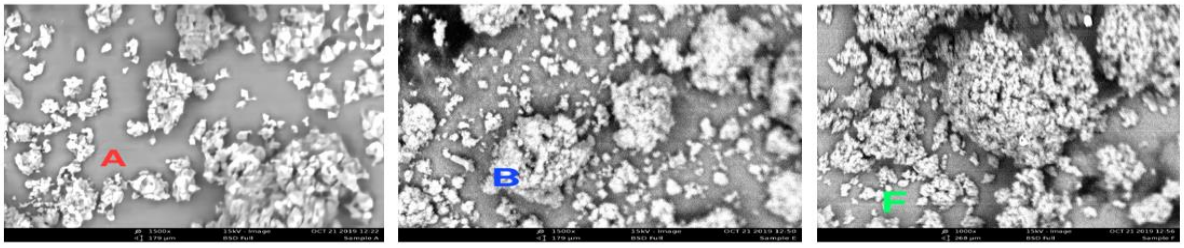

Figure 4: SEM Structure of PAni-pTSA samples A, B, and F

The oxidative chemical polymerization of aniline reported by Maity (2016) on the effect of reaction time and temperature resulted in the production of rod-like particles for 30 min polymerization time. As the polymerization is initiated by the APS, the oxidising agent, fibers are generated, followed by subsequent polymerization from these fibers, leading to the formation of irregularly shaped agglomerates. As a result, the polymerization product may include fibers as well as irregular agglomerates. A similar observation was made in this study (Figure 4). It is observed that rapid initiator addition, favours polymer initiation and primary growth, resulting in high fibers content in the product. In contrast, slow initiator addition or longer polymerization time favours secondary growth or the formation of globular particles, resulting in a more agglomerated morphology. Since the three rates of addition used in this research were all relatively gradual (30, 45, and 60 cm^3/h), both primary (fibers) and secondary (agglomerates) growth should be present in all of the samples. Some reports have claimed an increase in molecular weight with the decrease in polymerization temperature (Maity, 2006)

Reaction Optimization via Box-Behnken Design

Response surface regression analysis

Table 2 displays the runs and associated responses in the Box Behnken design. The reported percentage yield is the average of two yield measurements.

Table 2: Percentage Yield of Polyaniline

Run Order	X_1 (mol/dm^3)	X_2	X_3 (cm^3/hr)	Yield (%)
1	0.55	1.5	60	49.02
2	0.55	0.5	60	25.71
3	1.00	1.0	60	26.43
4	0.55	1.5	30	50.21
5	1.00	1.0	30	26.42
6	0.55	1.0	45	31.49
7	0.55	1.0	45	31.38
8	0.10	0.5	45	34.84
9	0.10	1.0	60	54.60
10	0.55	0.5	30	26.81
11	1.00	0.5	45	23.38
12	0.10	1.5	45	82.81
13	0.55	1.0	45	36.75
14	0.10	1.0	30	80.61
15	1.00	1.5	45	30.91

The yield regression equation was as follows:

$$\text{Yield } (\%) = 94.4 - 90.1\,X_1 + 47.6\,X_2 - 2.51\,X_3 + 46.6\,X_1^2 + 1.4\,X_2^2 + 0.0195\,X_3^2 - 44.9\,X_1{*}X_2 + 0.964\,X_1{*}X_3 - 0.003\,X_2{*}X_3 \quad (3.1)$$

The regression equation depicts the effects of three parameters on the yield of PAni. These parameters are: dopant concentration (X_1), I/M ratio (X_2), and rate of addition (X_3) as well as their interactions. The positive sign for the coefficients is indicative of a synergistic influence, whereas a negative sign suggests an antagonistic influence. The direct relationship of each parameter on the response, namely percentage yield, can be seen in this equation. The coefficient of determination, R^2, and modified R^2 values were used to determine the model's fitness. Considering the optimization aim of the research, higher R-squared values are favourable, signifying the model's proficiency in predicting responses. The adjusted R-squared factor affects the descriptive terms and rises whenever a new term is introduced, which serendipitously enhances the model more than expected. Unlike R-squared, the adjusted counterpart may assume negative values and will invariably remain less than or equal to R-squared. The computed R-squared stands at 97.21%, with the adjusted R-squared at 92.19%, indicating an inability of the model to predict approximately 5% of the variability in the percentage yield. Additionally, Table 2 shows that the relevance of each parameter's impact on a response is assessable through its corresponding p-value, and the computed coefficients and their respective p-values.

At the selected significance level of 0.1, a lower p-value implies greater confidence in the significance of the parameters regarding their influence on polymer yield. As a result, the linear terms of dopant concentration, I/M ratio, and rate of addition, as well as the quadratic term of dopant concentration x dopant concentration, and two of the interaction factors (dopant concentration with I/M ratio and dopant concentration with rate of addition) seem to be the most important factors in determining PAni yield. The I/M ratio x rate of addition interaction factor did not have a meaningful impact on the yield at the chosen level of significance since their p-values were greater than 0.1. These factors mean that the interaction model is significant and therefore worthy of further study. Equation 3.2 below represents the final regression equation for the yield, containing solely those terms that possess statistical significance.:

$$\text{Yield } (\%) = 94.4 - 90.1\,X_1 + 47.6\,X_2 - 2.51\,X_3 + 46.6\,X_1^2 - 44.9\,X_1{*}X_2 + 0.964\,X_1{*}X_3 \quad (3.2)$$

Table 3: PAni Yield Regression Analysis

Terms	Coefficients	p-Value	Remarks
Constant	94.4	0.000	Significant
Dopant Concentration	-90.1	0.020	Significant
I/M Ratio	47.6	0.156	Not Significant
Rate of addition	-2.51	0.090	Significant
Dopant Conc. x Dopant Conc.	46.6	0.020	Significant
I/M Ratio x I/M Ratio	1.4	0.905	Not Significant
Rate of addition x Rate of addition	0.195	0.177	Not Significant
Dopant concentration x I/M Ratio	-44.9	0.013	Significant
Dopant Conc. x rate of addition	0.964	0.060	Significant
I/M Ratio x Rate of addition	-0.003	0.994	Not Significant

Table 3 contains the calculated values for the coefficients of the parameters and their corresponding p-values. The peak areas of quinoid (A_Q), and benzoid (A_B) are shown in Table 3 with their relative ratios. It was observed that all the samples have their ratios near unity, suggesting approximately equal amounts of quinoid and benzoid groups in the PAni polymer

Effects of p-TSA concentration, I/M Ratio, and Rate of Initiator addition on the Yield

The plots depicting the main effects or interaction effects may be used to make inferences about the relationships between the variables and the responses. For PAni Yield, the analysis revealed an interaction effect between dopant concentration and I/M ratio and dopant concentration and rate of addition of initiator solution. As a result, as shown in Figures 5 and 6, main effect plots and interaction plots were used to describe the relationship between the variables mentioned above and PAni yield.

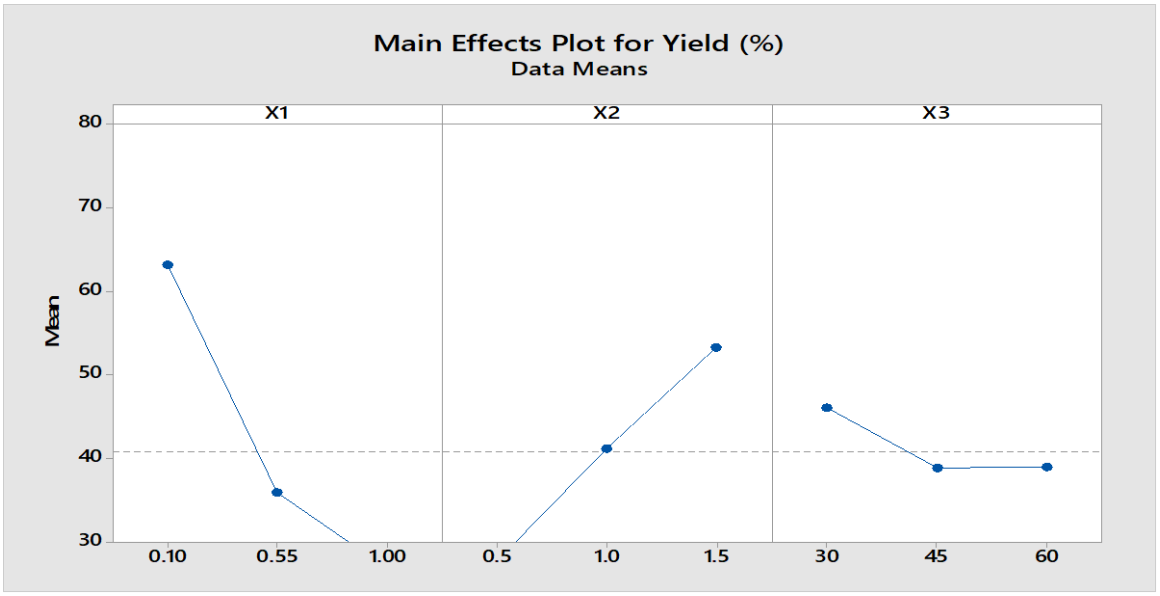

Figure 5: Main Effects Plots

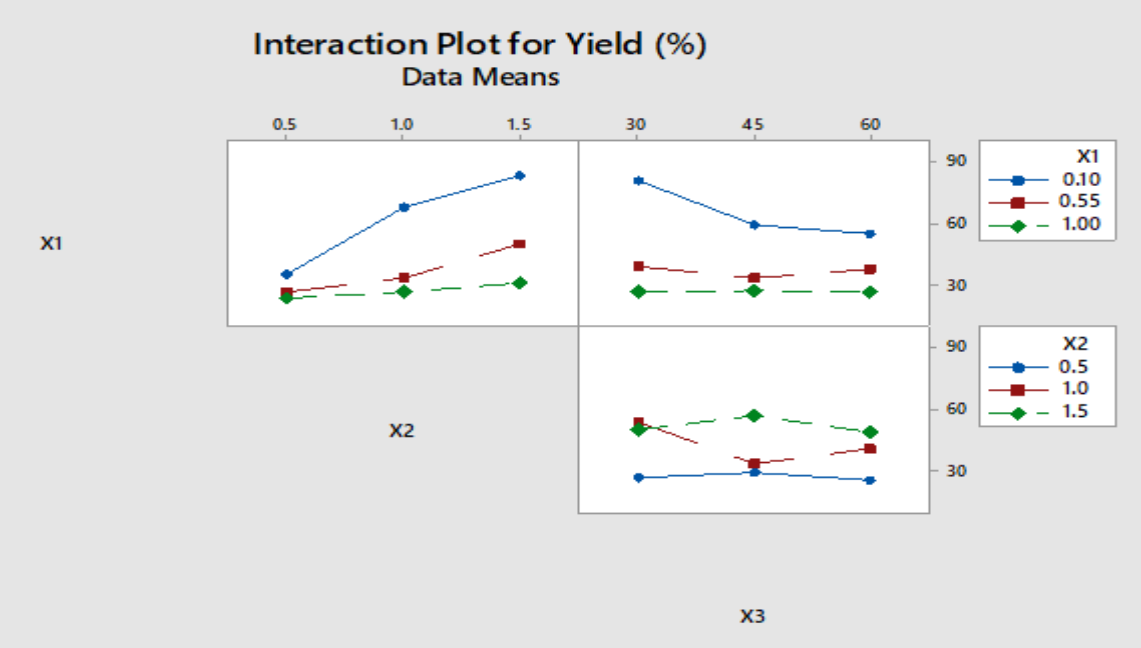

Figure 6: Interaction Plots

The value of the dopant concentration and the I/M ratio can be seen in the main effect plots (Figure 5) for the final yield of PAni. The yield was found to decrease as the dopant concentration was increased. The decreased yield at higher dopant acid concentrations may be due to an increased hydrolysis rate of the polyemeraldine chain or the formation of more micelle having a limited number of monomer particles, which results in the polymer's limited growth chain (Shah *et al.,* 2019). Small chain polymers are formed as a result, which were removed during washing with acetone.

The yield of PAni increased linearly as the I/M ratio increased up to 1.5, which was the maximum amount chosen for this experiment. It should be noted that further increase in the I/M ratio may result in over oxidation of radical cations, which is responsible for the growth rate and the chain length of the polymer. As a result, shorter polymer chains called oligomers are formed (Shah *et al.,* 2019). These oligomers were removed from the PAni product during the washing with acetone.

In the case of initiator concentration equimolar to aniline, a faster rate of reaction is observed due to the formation of a maximum number of anilinium radical cations. The yield was therefore found to be high. Also, the steady decrease of the initiator concentration results in a lower polymer yield due to successive decreases in radical cations' concentration. This is especially true in the present study as shown in Table 1. The effect of increasing the rate of addition of the initiator on the yield shows a linear decrease in the yield of up to 45cm^3/hr. More so, it was noted that when the factors; dopant concentration and addition rate of initiator are at a low value, and the I/M ratio is at a high value as shown in Figure 3.6, the yield reaches its maximum value. Also, a polymer with good properties such as solubility, thermal stability, and electrical conductivity would be formed.

Optimization Response surface and contour plots

The yield response surface diagram is shown in Figure 7 while the yield contour plots are shown in Figure 3.8. The dark green coloured area denotes the areas with the highest response. A dopant concentration below 0.1M and an intermediate I/M ratio (1.4 - 1.5) resulted in

achieving the highest yield of 80%, as illustrated in the graphical representation. Within the specified range of factors, the rate of initiator addition seems to exert negligible influence on the yield. Upon this observation, contours and surface plots were generated to analyze various combinations of the factorial levels selected in this study.

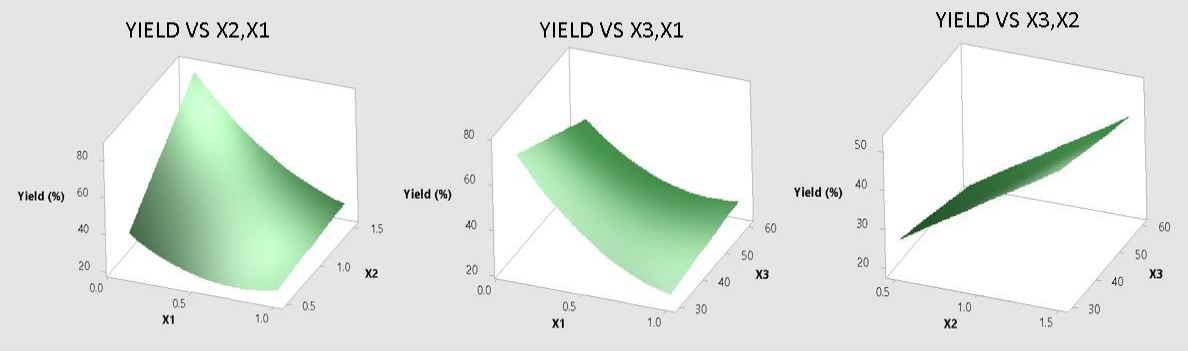

Figure 7: Response Surface Plots of Yield (%) vs (a) X_2,X_1 (b) X_3,X_1 (c) X_3,X_2

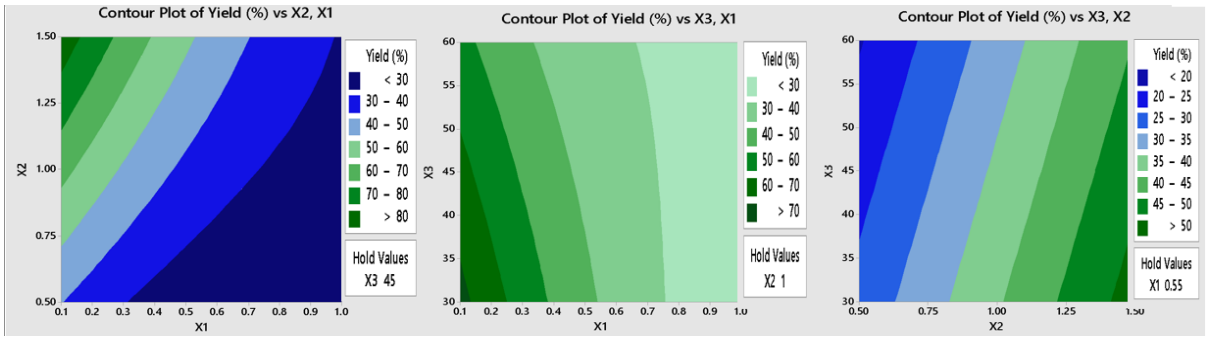

Figure 8: Contour Plot of Yield vs (a) X_2, X_1 (b) X_3,X_1 (c) X_3,X_2

Overlaid contour plots

The yield contour plot was overlaid to determine the desirable area for the yield. In Figure 3.9, the overlaid portion is the white area. Within the optimized area, any given factorial combination will yield the desired yield values. Three different rates of addition were overlaid on the plots.

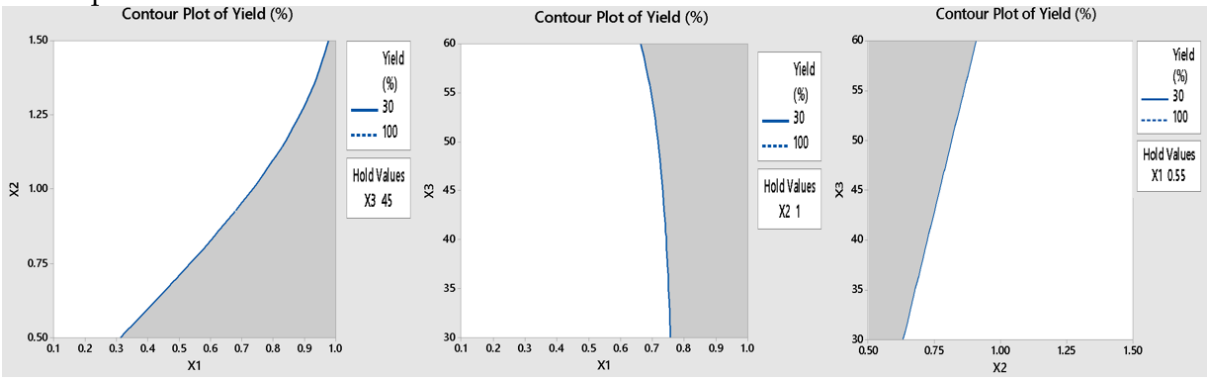

Figure 9: Overlaid Contour Plot of Yield (a) X_2,X_1 (b) X_3,X_1 (c) X_3,X_2

Validation Experiments

Table 3.4 indicates the results of the three (3) experimental runs carried out to validate the model. The X_1', X_2', and X_3' represent the dopant acid concentration, initiator-to-monomer

ratio, and addition rate of the initiator-to-monomer for the validation experiments respectively.

The validity of the model was verified through confirmatory experiments conducted using three data points situated within the experimental domain, which were separate from the initial fifteen data points. Among these, one data point coincided with the optimal prediction of the model (0.1M, 1.5 I/M, and 30 cm3/hr). The analysis presented in Table 3.4 demonstrates the comparison between predicted and observed values of yield, showcasing a notable agreement between the two sets of values and thereby affirming the adequacy of the model for yield optimization (Jelmy *et al.*, 2013).

Table 4: Comparison of Predicted and Observed Percentage Yield Values for Model Validation Experiment of PAni-pTSA

S/N	X_1'	X_2'	X_3'	Predicted (%)	Observed (%)	%Deviation
1	0.10	1.50	30	96.14	91.28	2.73
2	0.22	1.50	30	82.80	79.46	2.36
3	0.10	1.50	60.00	76.06	72.53	2.50

Optimization Plot for Yield

The most favorable yield values were determined through the utilization of MINITAB 17. Figure 3.10 illustrates the graphical representation of the optimal yield value. Within the experimental domain, the terms "high" and "low" depict the maximum and minimum values, respectively. MINITAB 17 specifies the desirability of the outcomes, typically ranging from 0 to 1, indicating the desired proximity between the predicted response and the target. Under the optimized conditions of a pTSA concentration of 0.10 mol/dm^3, an initiator addition rate of 30 cm^3/h, and an I/M ratio of 1.5, PAni with a yield of 96% was obtained.

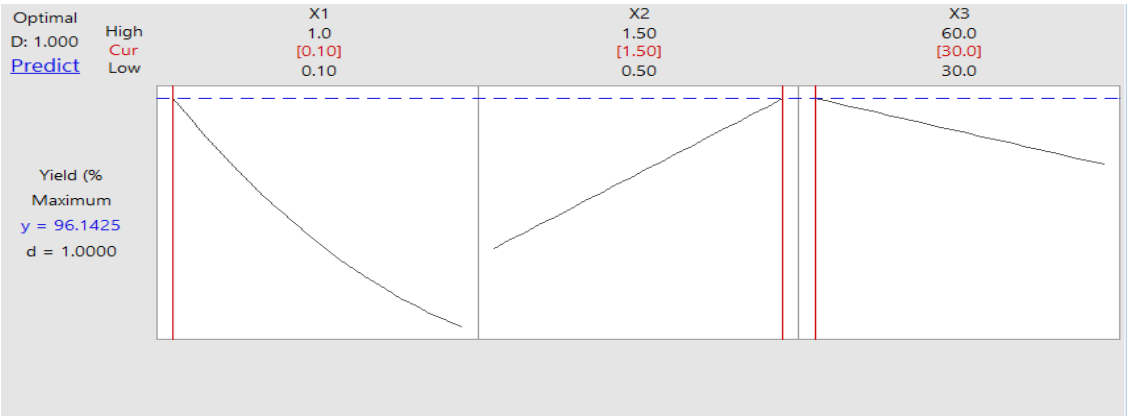

Figure 10: Yield Optimization Plots

The findings suggest that a higher concentration of aniline monomer generally corresponds to greater availability of initiator radicals, potentially enhancing the initiation of polymer chains and thus increasing the yield. However, excessively high concentrations of aniline may deplete the initiator radicals prematurely, resulting in shorter polymer chains and a reduced yield.

Similarly, a higher initiator-to-monomer ratio can lead to an increased yield by providing more initiator radicals for monomer initiation. Nonetheless, an excessive amount of initiator may trigger termination reactions between polymer chains, leading to a decrease in yield.

Additionally, the rate of initiator addition plays a crucial role, as a slower addition rate can promote controlled polymerization, facilitating the growth of longer polymer chains and potentially boosting the yield. However, overly slow addition rates may result in inefficient reactions and decreased yield.

Our observations indicate that the interplay between these factors is central to understanding the variation in yield across different experimental conditions. For instance, while a high concentration of aniline may be advantageous when accompanied by a sufficient initiator-to-monomer ratio, a slow rate of initiator addition could undermine this synergy by allowing excess aniline to prematurely consume the initiator radicals, thereby diminishing the yield. This complex interaction underscores the importance of carefully optimizing these parameters to achieve maximum yield in the synthesis of polyaniline.

The research findings suggest that the Box-Behnken Design of Experiments (DOE) can be employed to optimize the yield of polyaniline synthesis. This is achieved by taking into account the effects and interactions of various factors that influence the yield. By utilizing this approach, researchers can identify the most favorable conditions for producing polyaniline with a high yield. Jelmy *et al.* (2013) utilized this approach to optimize the conductivity and yield of polyaniline synthesis, while Hamtak *et al.* (2023) applied it to optimize the synthesis of polyaniline-polypyrrole composite for corrosion protection of carbon steel. Their findings validate the effectiveness of the method for optimizing the yield of Polyaniline.

CONCLUSION

The yield of PAni polymer was optimized using the Box Behnken design of the experiment approach. The polymer maximum yield obtained is 82.81 percent when the dopant acid concentration is 0.1 mol/dm^3, the initiator addition rate is 45 cm^3/h, and the I/M ratio is 1.5. The experiments conducted for validation affirmed the predicted yield and validated the appropriateness of the selected model. The percentage yield of the PAni-pTSA was affected by the factors chosen, according to characterization studies on three representative samples chosen from the DOE experimental runs. The FTIR studies established the form of the synthesized PAni. The semi-conductive feature of the synthesized PAni was validated by the properties seen in the UV-Vis. This implies that the synthesized PAni could be a potential candidate for the development of anticorrosive properties of a two-pack epoxy coating system. Semi-conductive PAni could enhance the coating's ability to shift electrical potentials and create a less hospitable environment for rust and decay. This leads to longer-lasting protection for structures and equipment in harsh conditions.
The chemically synthesized polyaniline doped with p-toluene sulfonic acid (pTSA) is being investigated as an anticorrosion agent in an offshore setting in a two-component epoxy paint coating system.

REFERENCES

Aizamddin, M. H., Roslan, N. C., Kamarudin, M. A., Omar, S. N. I., Safian, M. F., Halim, M. I. A., & Mahat, M. M. (2020). Study of conductivity and thermal properties of polyaniline doped with p-toluene sulfonic acid. *Malaysian Journal of Analytical Sciences*, 24(3), 413-421.

Bavane, R. G. (2014). Synthesis and characterization of thin films of conducting polymers for gas sensing applications [Doctoral dissertation, Savitribai Phule Pune University]. http://hdl.handle.net/10603/48043

Haldhar, R., Asrafali, S. P., Raorane, C. J., Periyasamy, T., & Kim, S. C. (2022). Performance of cross-linked polymers as a potential anticorrosive coating for low carbon steel in acidic

condition: Experimental and computational studies. *Journal of Molecular Liquids*, 360, 119384. https://doi.org/10.1016/j.molliq.2022.119384

Jelmy, E. J., Ramakrishnan, S., Devanathan, S., Rangarajan, M., & Kothurkar, N. K. (2013). Optimization of the conductivity and yield of chemically synthesized polyaniline using a design of experiments. *Journal of Applied Polymer Science*, 130(2), 1047–1058. https://doi.org/10.1002/APP.39268

Hamtak, M., Barzegar Khaleghi, M. H., Sajjadnejad, M. (2023). 'Optimized synthesis of polyaniline-polypyrrole composite for corrosion protection of carbon steel', *Materials Chemistry and Mechanics*, 1(1), pp. 58-67.

Khalid, M., Maria, A., Honorato, B. & Varela, H. (2011). Polyaniline: Synthesis methods, doping, and conduction mechanism. In Polyaniline - from synthesis to practical applications (pp. 1-17). IntechOpen. https://doi.org/10.5772/intechopen.79089

Li, X. (2018). Preparation, properties, and application of polyaniline nanocomposites. *Chemical Engineering Transactions*, 71, 889-895. https://doi.org/10.3303/CET1871149

Luscombe, C. K., Maitra, U., Walter, M., & Wiedmer, S. K. (2021). Theoretical background on semiconducting polymers and their applications to OSCs and OLEDs. *Chemistry Teacher International*, 3(2), 169–183. https://doi.org/10.1515/cti-2020-0020

Maity, P. C., & Khandelwal, M. (2016). Synthesis time and temperature effect on polyaniline morphology and conductivity. *American Journal of Materials Synthesis and Processing*, 1(4), 37-42.

Mishra, A. K. (2018). Conducting polymers: Concepts and applications. *Journal of Atomic, Molecular, Condensate and Nano Physics*, 5(2), 159-193. https://doi.org/10.26713/jamcnp.v5i2.842

Rafeeq, S. N. & Khalaf, W. Z. (2015) Preparation, characterization and electrical conductivity of doped polyaniline with (HCl and pTSA). *Engineering & Technology Journal*, 33(Part B7), pp. 1220-1231.

Ratheesh, R. & Vishwanathan, K. (2013) Calorimetric and thermogravimetric studies in para toluene sulphonic acid (pTSA) doped poly(aniline). *International Journal of Scientific Research*, 2(11), pp. 466-468.

Shah, A., Kamran, M., Bilal, M., & Ullah, R. (2019). Cost-effective chemical oxidative synthesis of soluble and electroactive polyaniline salt and its application as anticorrosive agent for steel. *Materials*, 12(9), 1527. https://doi.org/10.3390/ma12091527

Sharma, A. & Sharma, S. (2023) Graphene-based polymer coatings for preventing marine corrosion: A review. *Journal of Coatings Technology and Research*. https://doi.org/10.1007/s11998-022-00730-x

Sharma, S., Sudhakara, P., Omran, A. A. B., Singh, J. & Ilyas, R. A. (2021) Recent trends and developments in conducting polymer nanocomposites for multifunctional applications. *Polymers*, 13(17), 2898. https://doi.org/10.3390/polym13172898

Sinha, S., Bhadra, S. & Khastgir, D. (2009) Effect of dopant type on the properties of polyaniline. *Journal of Applied Polymer Science*, 112(5), pp. 3135-3140. https://doi.org/10.1002/app.29708

Ulaeto, S. B., Ravi, R. P., Udoh, I. I., Mathew, G. M. & Rajan, T. P. D. (2023) Polymer-based coating for steel protection, highlighting metal-organic framework as functional actives: A review *Corrosion and Materials Degradation*, 4(2), pp. 284-316. https://doi.org/10.3390/cmd4020015